16th World Conference on Earthquake, 16WCEE 2017

Santiago Chile, January 9th to 13th 2017

Paper N° 2548

Registration Code: S-R1463496430

EXPERIMENTAL DYNAMIC RESPONSE OF FREE-STANDING BODIES UNDER NEAR FIELD AND FAR FIELD GROUND MOTIONS

S. Dangol(1), A. Maree(2), T. Nielsen(2), L. Ibarra(3), D. Sanders(4), C. Pantelides(5)

(1) *Graduate Student, University of Utah, sharad.dangol@utah.edu*
(2) *Graduate Student, University of Nevada at Reno, ahfarghal@nevada.unr.edu; taylorn@nevada.unr.edu*
(3) *Assistant Professor, University of Utah, luis.ibarra@utah.edu*
(4) *Professor, University of Nevada at Reno, sanders@unr.edu*
(5) *Professor, University of Utah, c.pantelides@utah.edu*

Abstract

This study is a part of a research project evaluating seismic response of free-standing dry storage casks under long-term seismic events. Free-standing structures are highly susceptible to rocking and sliding during seismic events. Characterization of motion of three dimensional free-standing structures is a highly nonlinear problem, especially when rocking and sliding motion occur simultaneously. Response of such free-standing bodies depend on many factors like aspect ratios (radius to centroidal height ratio, r/hcg), coefficient of friction and ground motion characteristics. The main purpose of this article is to present the effect of ground motions with a single large pulse and those with multiple smaller pulses (NFGMs and FFGMs, respectively) on the dynamic response of free-standing bodies. For this purpose, experiments with Near Field and Far Field ground motions were conducted using a six degree-of-freedom (6DOF) shake table at the University of Nevada, Reno. Four scaled free-standing bodies with four different aspect ratio: 0.39, 0.43, 0.55 and 0.62; were studied in the experimental tests. However, results for free-standing bodies of three aspect ratios (0.39, 0.43, and 0.62) are discussed in this article. Ground motion records used in the study were spectrally matched to the seismic hazard level or spectral accelerations developed for earthquake events of 10,000 and 30,000 year return periods. The same system and ground motion cases were used several times to investigate whether the response of free-standing bodies is repeatable under scenarios. The experimental results show that the ground motions containing multiple pulses (FFGMs) produces more lateral displacements and rocking angle compared to NFGMs. The results also show that the casks' response lacks repeatability under random ground motions. Finally, three chaotic analysis methods are used to investigate the reason behind such lack of repeatability.

Keywords: Free-standing Structures; Rocking; Sliding; Near Field and Far Field Motion; Chaotic analysis

1. Introduction

Free-standing structures are not anchored to their foundation or supporting base, and are highly susceptible to rocking and sliding during seismic events. Excessive sliding of such bodies may lead to impact with adjacent structures, whereas rocking may result in overturning or tip-over. For certain applications, such as storage of spent nuclear fuel rods, these scenarios can lead to unacceptable system performance. Motion of three dimensional free-standing structures is a highly nonlinear problem [1–3], especially when rocking and sliding motion occur simultaneously. Response of such free-standing bodies depend on many factors like aspect ratios (radius to centroidal height ratio, r/hcg), coefficient of friction, ground motion characteristics [4]. This study is a part of a research project evaluating seismic response of free-standing dry storage casks (DSCs) under long-term seismic events and investigates the effect of ground motion characteristics on the response of free-standing structures.

One of the initial studies of free-standing body's response was conducted by Housner in 1963 [5], a work followed by several studies on rigid blocks [1,2,6,7]. Most studies, however, simplify the problem by focusing only on pure rocking of planar rigid bodies (two dimensional blocks, 2D), with few exceptions [7]. Also, while most of these studies deal with numerical modelling of 2D and 3D rigid block type structures, there is a lack of experimental tests on free standing bodies; especially on cylindrical free-standing bodies, such as unanchored DSCs used to store spent nuclear fuel. This study attempts to present the effect of near field and far field ground motions (NFGMs and FFGMs, respectively), on the response of cylindrical free-standing bodies. For this purpose, experimental tests were conducted using a six degree-of-freedom (6DOF) shake table at the University of Nevada, Reno. Experiments were carried out for ground motions that with NFGM as well as FFGM characteristics. Free-standing bodies of four aspect ratios (radius to centroidal height ratio, r/hcg) were studied: 0.39, 0.43, 0.55 and 0.62. Ground motion records used in the study were spectrally matched to the seismic hazard level or spectral accelerations developed for earthquake events of 10,000 and 30,000 year return periods [8,9]. Experimental tests under repeated ground motion were also carried out several times to investigate whether the response of free-standing bodies is repeatable.

2. Evaluated system

2.1 Free-standing bodies (DSCs) characteristics

Two DSC scaled models with aspect ratios (radius-to-centroidal height, r/h_{cg}) of 0.55 (Cask I) and 0.43 (Cask II) were initially considered, ratios that correspond to the lower bound and average aspect ratios of Nuclear Regulatory Commission (NRC) approved casks [4], respectively. Although the main physical characteristics of these generic DSCs are based on NRC list, the detailed dimensions of the overpack and multi-purpose canister (MPC) do not correspond to commercially available casks. The specimens were assumed to be 1:2.5 scale models of a generic prototype. The slender cask with aspect ratio of 0.43 is more likely to exhibit large rotations, whereas the squat cask with aspect ratio of 0.55 is more likely to show sliding displacements. The similarity law between the scaled and prototype casks are given in Table 1.

Two additional specimens of aspect ratio 0.39 and 0.62 were also tested. Theses specimen were considered to be scaled at 1:3.5. It has to be noted that second specimen (r/h_{cg} = 0.62) is too light to be considered as true 1:3.5 scaled. However, the applied ground motions' time step was scaled considering 1:3.5 scale. The first specimen was MPC only of the Cask I (named Cask I-M) and the second specimen was empty overpack of Cask I, without the additional mass filling and MPC (named Cask I-O). These two specimens represent reasonable extremes of NRC free-standing cask's aspect ratios. An advantage of using relative light weight casks is that that larger input accelerations could be experimentally applied. Dimensional details of all the specimens are presented in Table 2, whereas Fig. 1a shows the overpack of the scaled prototype DSC. The overpack cavity and the canister (Figs. 1c and 1d) was filled with lead units (Fig. 1b) to compensate for the additional mass necessary to satisfy the similitude law [10]. The lead units were welded together at the top to prevent pounding. The leftover space of MPC and overpack cavity was filled with sand. Table 2 presents dimensional details for all the specimen casks. The intensity of ground motions successfully applied to Cask I were too small to produce significant cask displacements, and these results are not presented in this paper.

Table 1: Similarity law for scaled specimens

Parameter	Notation	Dimension	Similarity Ratio		
			General Form*	N = 2.5	N = 3.5
Length	L	L	$L_s/L_p = 1/N$	1/2.5	1/3.5
Time	T	T	$T_s/T_p = 1/N^{1/2}$	0.6325	0.5345
Acceleration	a	LT^{-2}	$a_s/a_p = 1$	1	1
Angle	θ	---	$\theta_s/\theta_p = 1$	1	1
Mass	M	M	$M_s/M_p = \alpha(1/N^3)$	0.16	0.0816
Mass Moment of Inertia	I	ML^2	$I_s/I_p = M_sL_s^2/M_pL_p^2=\alpha(1/N^5)$	0.0256	0.0067
Equivalent Cross Section	A	L^2	$A_s/A_p = 1/N^2$	0.16	0.0816
Bottom Stress	σ	$ML^{-1}T^{-2}$	$\sigma_s/\sigma_p = (M_sa_s/A_s)/ (M_pa_p/A_p)=1$	1	1
Friction Coefficient	μ	---	$\mu_s/\mu_p = 1$	1	1
(*) Suffix (p) refers to generic prototype, and suffix (s) refers to scaled model specimens α = correction factor = N					

Table 2: Dimensions of 1:2.5 scaled casks

DSC Specimen	Component	Diameter (mm.)	Height (h, mm.)	Weight (ton)	Scale
Cask I (r/h_{cg} = 0.55)	MPC	660	1765	4.8	1:2.5
	Overpack	670 (inside) 1156 (outside)	1786 (cavity) 2223 (total)	11.96	
Cask II (r/h_{cg} = 0.43)	MPC	660	1867	5.05	1:2.5
	Overpack	670 (inside) 1054 (outside)	1880 (cavity) 2426 (total)	9.72	
Cask I-M (r/h_{cg} =0.39)	MPC	660	1765	4.8	1:3.5
Cask I-O (r/h_{cg} = 0.62)	Empty overpack only	1156 (outside)	2223 (total)	3.39	1:3.5

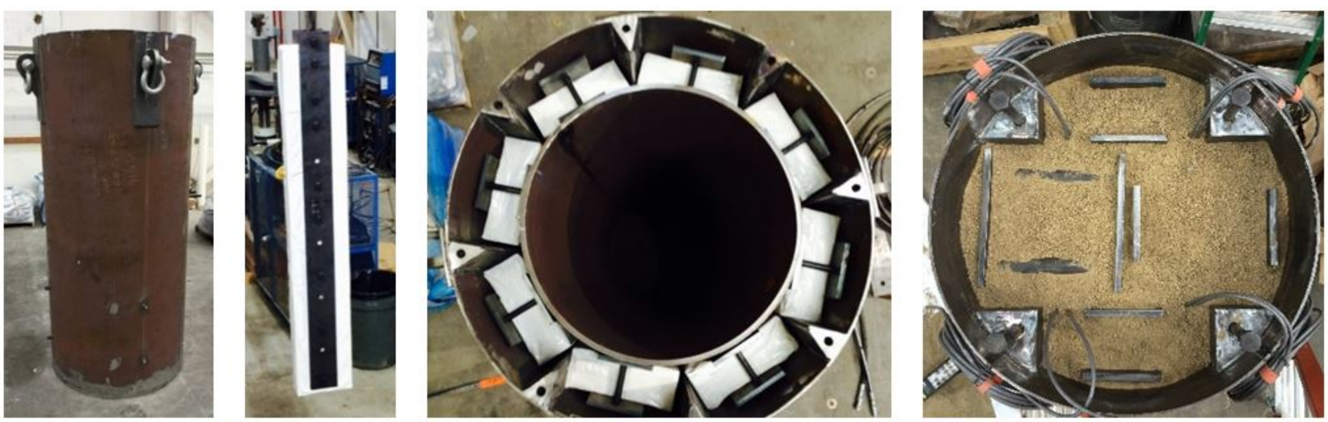

(a) (b) (c) (d)

Fig. 1 – (a) Cask II's overpack, (b) Assembly of lead units in one panel, (c) Overpack cavity filled with lead, and (d) MPC filled with lead and sand

2.2 Ground Motions

Ground motions can be broadly classified as near field or far field ground motions. NFGMs need to be recorded close to the fault and exhibit forward directivity. The main characteristic of NFGMs is that they contain one or two major pulses. FFGMs are recorded relatively far from the fault and contain multiple pulses. As the research project's goal is to evaluate the seismic response of DSCs under long term seismic event, NFGMs and FFGMs were spectrally matched to target spectra of 10,000 and 30,000 years. Fig. 2 presents the target response spectra developed for respective return periods for western US rock. The target spectra were developed using methods outlined in NUREG 6728 [8] and spectral matching was done using a computer program RSPMATCH [9]. Long return period GMs are considered because the increase in the DSC compliance period from 20 to 300 years would increase the return period from 2,000 to 29,850 years to preserve the same probability of exceedance of 1% during the compliance period [11].

Two ground motion sets (one for NFGM and FFGM each) were selected and spectrally matched to the seismic hazard level or spectral accelerations (Fig. 2). NFGM are events with magnitude M = 6 and distance R = 2 km, while FFGM were developed with M = 8 and R = 20 km. From the ground motion sets, two representative spectrally matched ground motions were selected as the input for the seismic excitation test. Table 3 presents the ground motions used as input for the test and PGA for each at respective return period. Fig 3 shows the time histories for spectrally matched motions (10,000 year return period), whereas Fig. 4 presents the time histories for ground motions spectrally matched to 30,000 year target spectra. Figs 3 and 4 also show the significant duration for the ground motions based on Arias intensity. The significant duration represents the strong shaking duration, and it denotes the timespan in which a specified amount of energy is dissipated. In this case, this timespan corresponds to the occurrence of 5% and 95% of the total Arias intensity. For the selected FFMG, the significant duration is approximately three times (about 30 s.) larger than that of the NFGM record.

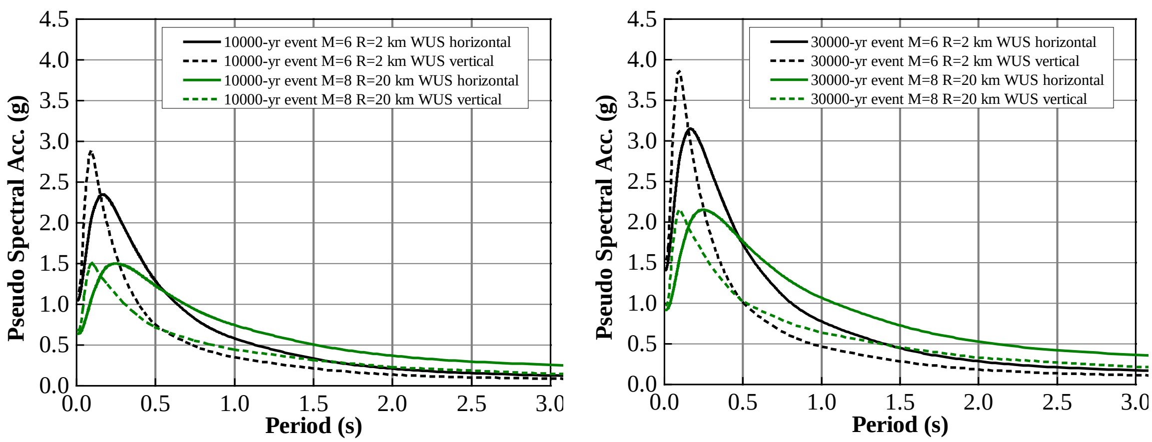

(a) (b)

Fig. 2 – Target response spectra developed for western US rock: (a) 10,000 year event; (b) 30,000 year event

Table 3: Peak Ground Accelerations (PGAs) of target spectra

Earthquake Name	Year	Station	Target Spectrum		Peak Ground Acceleration (PGA), g		
					Original	10,000 yr. return period	30,000 yr. return period
Erzican, Turkey	1992	Erzican	NFGM	Horizontal	EW 0.496, NS 0.515	1.053	1.412
				Vertical	0.248	1.127	1.511
Chi-Chi, Taiwan	1999	CHY101	FFGM	Horizontal	EW 0.353, NS 0.440	0.640	0.918
				Vertical	0.165	0.685	0.982

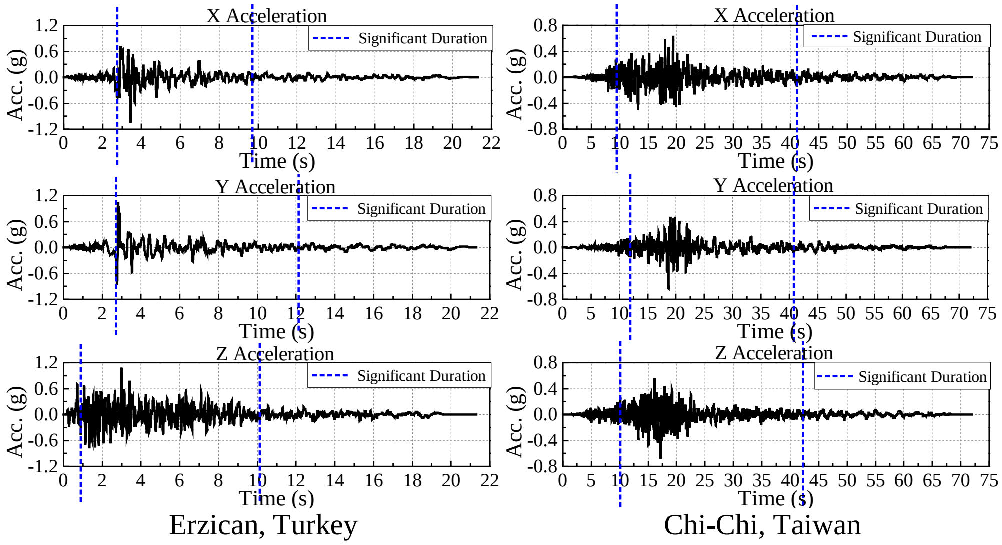

Fig. 3 – Time histories of input ground motions spectrally matched to 10,000 year return period

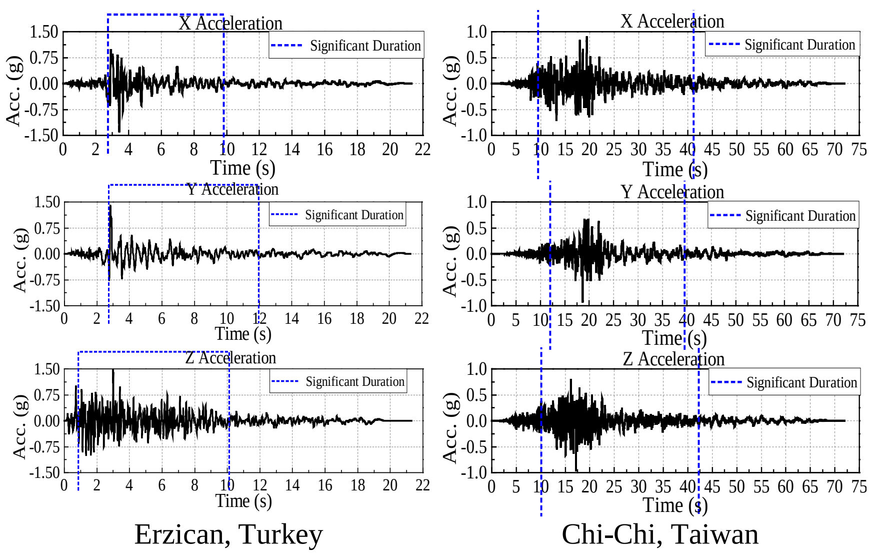

Fig. 4 – Time histories of input ground motions spectrally matched to 30,000 year return period

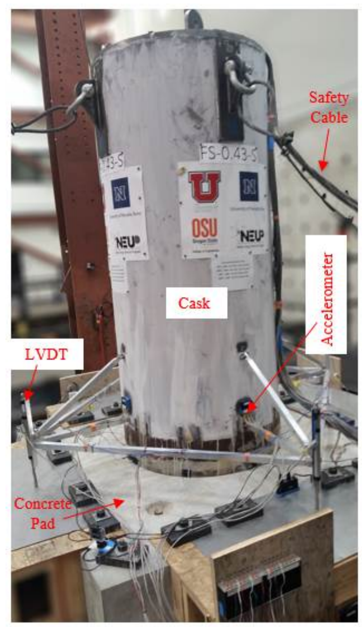

Fig. 5 – Experimental test setup of free-standing cask

3. Experimental test setup

Fig. 5 shows the experimental setup of the cask on top of a concrete pad of dimensions 2,134 mm × 2,134 mm × 354 mm. The pad is anchored to the 6-degree-of-freedom shaking table, while the cask is free standing on top of the concrete pad. To prevent damage due to a potential tip-over, a safety cable system was implemented during the tests. The ground motions presented in Figs. 3 and 4 were applied to the scaled cask at different magnitude incremental steps, until the shake table was automatically stopped when the impact forces exceeded the allowable load capacity of the vertical actuators, or the vertical displacements at the edge of the cask exceeded 101. 6 mm. The maximum intensity of ground motions that could be applied for testing of Casks I and II are given in Table 4. Cask I, under the respective ground motions, did not show significant movement because of the low accelerations of the maximum applied ground motions. Hence experimental results for Cask I are not presented in this paper. Cask I-M and Cask I-O were tested in a similar way. However, due to their relative light weight, larger magnitude of the ground motions (Figs. 3-4) could be applied. Maximum input motions for Cask I-M are also given in Table 4. Table 4 also presents the maximum intensity of ground motions applied for the test of Cask I-O.

Table 4: Intensity of Ground Motion Applied during Experimental Tests

Specimen	Ground Motion	Return Period (years)	Applied Intensity (%)	Target Scaled PGA (g)		
				X	Y	Vert. (Z)
Cask I	Erzican	10,000	30	0.316	0.316	0.338
	Chi-Chi	10,000	50	0.320	0.320	0.343
Cask II	Erzican	10,000	50	0.527	0.527	0.564
	Chi-Chi	10,000	75	0.480	0.480	0.514
Cask I-M	Erzican	10,000	75	0.790	0.790	0.845
	Chi-Chi	10,000	75	0.480	0.480	0.514
Cask I-O	Erzican	10,000	100	1.053	1.053	1.127
	Chi-Chi	10,000	100	0.640	0.640	0.685
	Erzican	30,000	75	1.059	1.059	1.133
	Chi-Chi	30,000	100	0.918	0.918	0.982

4. Experimental tests results

Fig. 6 show the response of Cask II for 50% of 10,000 year Erzican and 75% of 10,000 year Chi-Chi. Note that 10,000 year Chi-Chi at 75% has the smaller PGA of the two motions, but it led to the higher peak lateral displacements and rocking angle, possibly because this FFGM contains multiple pulses and it is able to sustain rocking and nutation motion of the cask. In this type of motion, the cask rolls or tumbles around its edge. During prolonged rocking and nutation, it is easier for cask to move around, producing larger displacements.

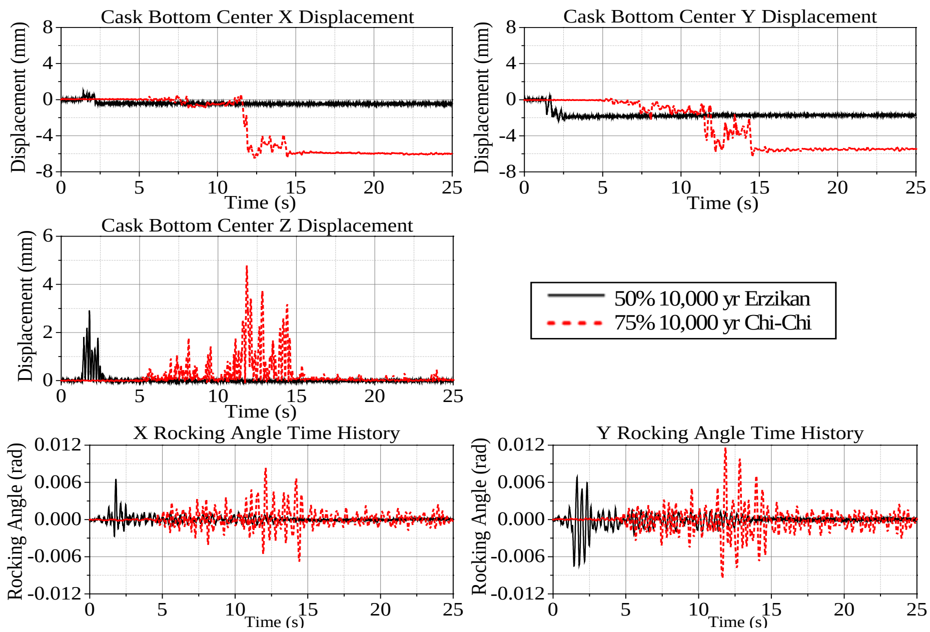

Fig. 6 – Response of Cask II 50% of 10,000 year Erzican and 75% of 10,000 year Chi-Chi

The experimental responses of Cask I-M for 75% of 10,000 year Erzican and 75% of 10,000 year Chi-Chi are shown in Fig. 7, indicating that rocking angle response increases as the aspect ratio decreases i.e., as the cask becomes slender. The results again indicate that sustained rocking and nutation motion are undesirable as it facilitates large lateral displacements. Unlike Cask II experimental tests, it has to be noted that, PGAs for applied magnitude of 10,000 year Erzican was considerably higher than that for 10,000 year Chi-Chi (Table 4). That resulted in larger rocking for the NFGM (Erzican). However, Chi-Chi still produced lateral displacements comparable to that resulted by Erzican. The response for Cask I-O under 100% of 10,000 year Erzican and 100% of 10,000 year Chi-Chi is presented in Fig. 8, whereas the response of 75% of 30,000 year Erzican and 100% of 30,000 year Chi-Chi is shown in Figs. 9. These figures suggests although NFGMs have larger PGAs, FFGM with multiple pulses produce more rocking and displacements.

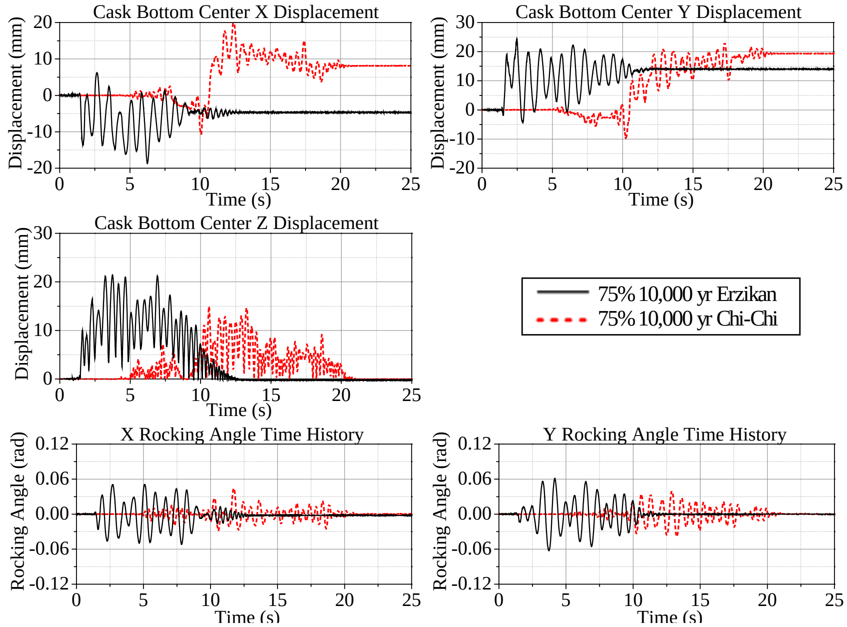

Fig. 7 – Response of Cask I-M under 75% of 10,000 year Erzican and 75% of 10,000 year Chi-Chi

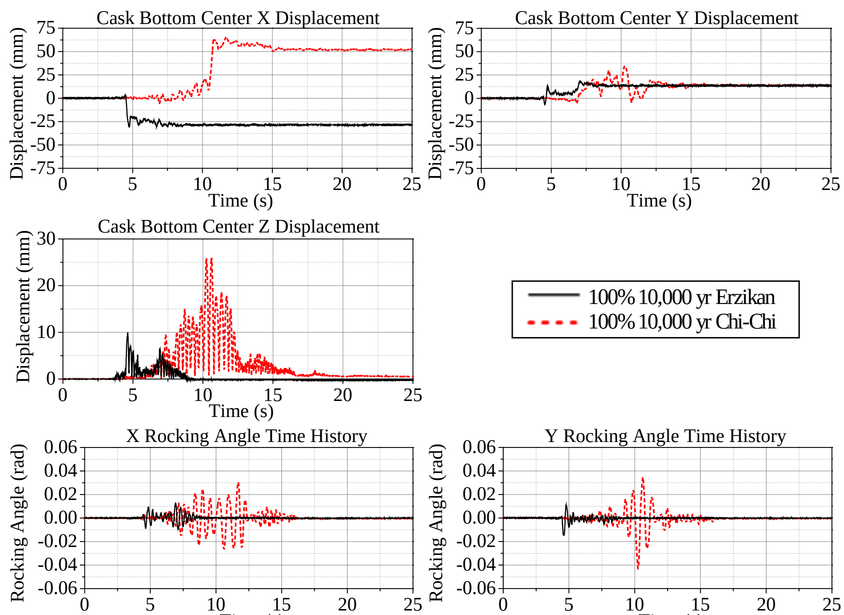

Fig. 8 – Response of Cask I-O under 100% of 10,000 year Erzican and 100% of 10,000 year Chi-Chi

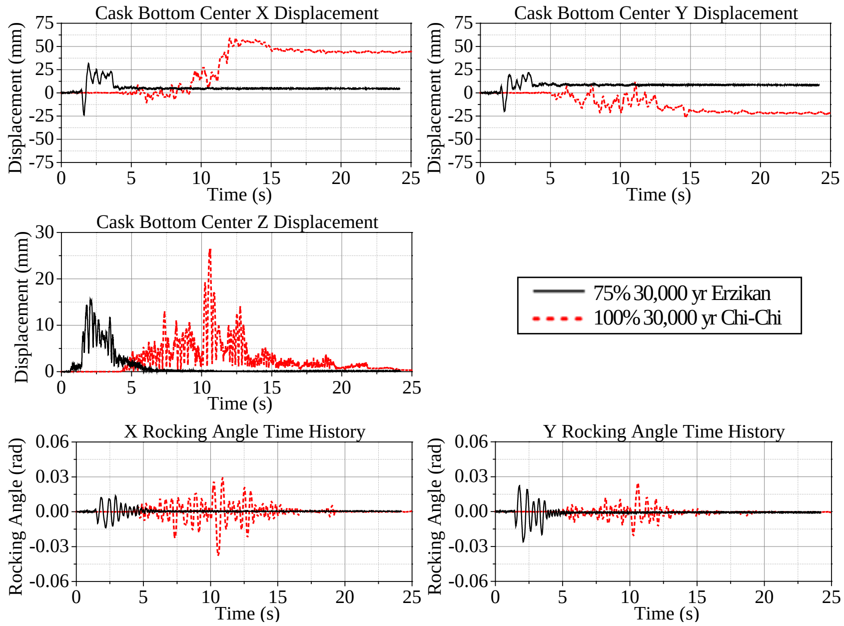

Fig. 9 – Response of Cask I-O under 75% of 30,000 year Erzican and 100% of 30,000 year Chi-Chi

5. Response under repeated motion

To investigate the response of free-standing casks under repeated seismic loading, casks were tested under the same ground motion multiple times. The lack of repeatability in the response of free-standing blocks has been known for a long time now. Yim et al. [6] suggested that responses of an object (even for rocking only motion) may deviate with minute changes in the system parameters or excitation details. This finding was confirmed experimentally by Aslam et al. [12]. They showed that depending on certain system and excitation parameters, the experiments were not repeatable. Hogan [13] furthered these studies and performed numerical study of rigid block under harmonic excitation to show the existence of many responses including subharmonic and chaotic response. Recently, Jeong et al. [14] carried out a numerical investigation on the effect of sliding, in addition to rocking, on the response of free standing planar bodies. They also conclude that under certain conditions rocking motion is chaotic and that sliding induces chaotic response in a rocking system. Experimental tests on free-standing blocks [15] also indicate that the response under random ground motions are not repeatable. Due to the highly nonlinear nature of such free-standing bodies, minute changes in the initial condition or boundary condition may result in very different movement of the body. While most of these previous study focuses on rigid “block” type structure, this study focuses on cylindrical free-standing bodies are more likely to exhibit higher sensitivity and chaotic response specifically in the lateral and rocking displacements of the system when it rocks, slides and tumbles along its edge.

This section presents the responses Cask I-M and Cask I-O under repeated ground motion. Cask I-M was subjected to four repeats of 75% 10,000 year Chi-Chi. Cask I-O was tested under 100% of 10,000 year Chi-Chi five times. Note that during each repeat test, the testing condition was not exactly the same. Minor differences do exist like shake table not being able to reproduce the exact same motion and minor changes in starting position among others. But these minor changes lead to very different cask response. Fig. 10 presents the response for repeat tests for Cask I-M. Lastly, Fig. 11 presents the response comparison for the five repeat test for Cask I-O, showing that free-standing DSC response lacks repeatability. As can be seen, the variation in response is more evident in the cask lateral displacement of the cask more than in its rocking response. Differences in time history of rocking angles, however, do exists. This apparent lack of repeatability in response might be due to small changes in initial conditions, boundary condition in combination with high frequencies contained within the applied ground motions. This lack of repeatability might make the prediction of lateral displacements particularly more difficult (more than the rocking response) using any computational tools like FEM and numerical models.

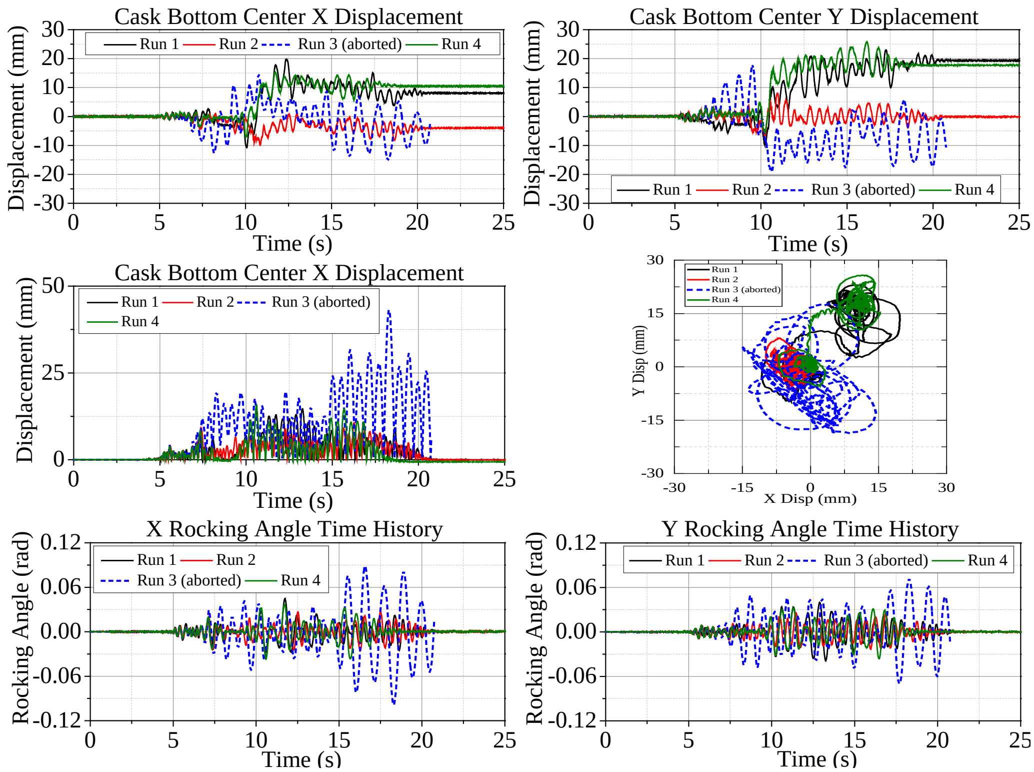

Fig. 10 – Comparison of Cask I-M response under repeated 75% of 10,000 year Chi-Chi

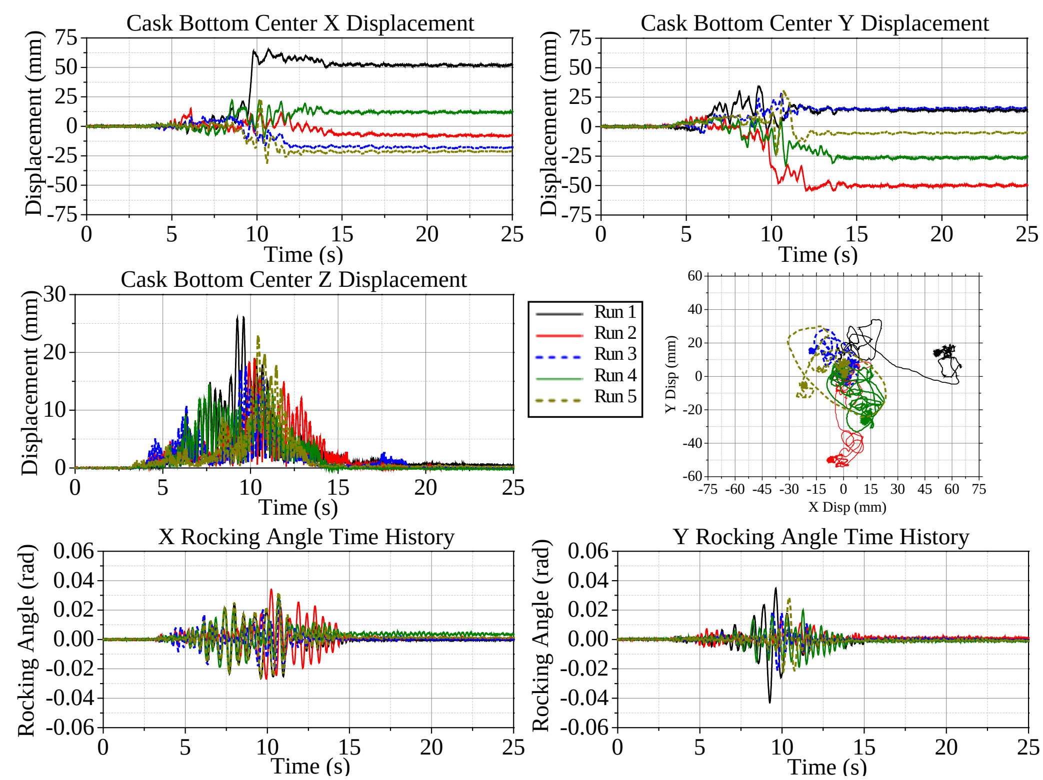

Fig. 11 – Comparison of Cask I-O response under repeated 100% of 10,000 year Chi-Chi

5.1 Chaotic response of DSCs specimens

The lack of repeatability observed in the experimental tests suggested the presence of chaotic response. This section summarizes three methods used to detect chaotic behavior on the pure rocking response of Cask I and Cask II: i) phase-space plot, ii) Fourier spectra, and iii) Poincaré sections. Each one of these approaches can indicate the potential presence of chaos in the rocking response. Chaotic analysis methods determine if the system's response is non-harmonic and/or non-periodic when subjected to a harmonic excitation.

Phase-space plot is the continuous plot of angular displacement versus angular velocity over time. Periodic motions are characterized by closed orbits in phase plane (phase-space) [14,16]. An indication of possible existence chaos is an open ended (discontinuous) or non-repeating phase-space plot. In other words, chaotic motions will have orbits that never close or repeat. Another clue of existence of chaos is the appearance of a broad spectrum of frequencies in the output, even though the input is a single frequency harmonic motion. The frequency spectrum in the output can be observed in an output Fourier Spectrum or Power Spectrum. Another indication of existence of chaos can be obtained from Poincaré section or map, which is a plot of points from the phase plane plot, sampled at discrete intervals. Instead of plotting the orbits in a continuous motion, in Poincaré section or map, points of the orbit are plotted at the dynamics at discrete times. This means the motion appears as a sequence of dots in phase plane. For a harmonic, subharmonic or period system, the Poincaré map or section would consist of set of finite number of points or a closed loop(s). For chaotic systems the map will not show such finite number of points and closed loop(s), but would rather show points distributed in wide space and/or forms strange attractors.

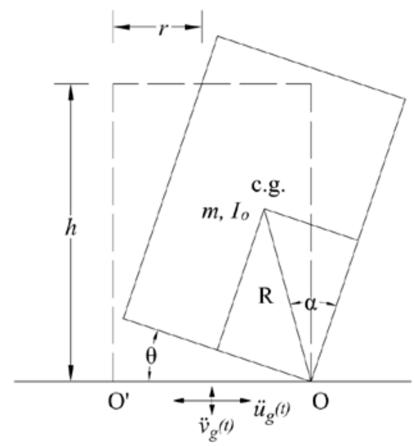

Fig. 12 – 2D rocking body

The pure rocking equation of motion for the 2D rocking body of Fig. 12. is given by Eq. (1) [2].

$$\ddot{\theta} = -p^2 \left\{ \sin[\alpha * \text{sgn}(\theta(t)) - \theta(t)] \left(1 + \frac{\ddot{v}_g}{g}\right) + \frac{\ddot{u}_g}{g} \cos[\alpha * \text{sgn}(\theta(t)) - \theta(t)] \right\} \tag{1}$$

where, $p = \sqrt{mgR/I}$ = frequency parameter; sgn(x) is a signum function; $R = \sqrt{r^2 + h_{cg}^2}$; $I = I_0 + mR^2$ = mass moment of inertia about rocking pole; $\alpha = \tan^{-1}(r/h_{cg})$ = critical angle; $\ddot{u}_g$ and $\ddot{v}_g$ are horizontal and vertical sinusoidal excitations, given by Eqs. (2) and (3) respectively.

$$\ddot{u}_g(t) = A_h \alpha g \sin(\omega t + \psi) \tag{2}$$

$$\ddot{v}_g(t) = A_v \alpha g \sin(\omega t + \psi) \tag{3}$$

$$\begin{aligned} \dot{\theta}_{i+1} &= e * \dot{\theta}_i \\ e &= 1 - \frac{2mR^2}{I} \sin^2 \alpha \end{aligned} \tag{4}$$

where, $A = a_p/(\alpha g)$ = normalized amplitude and $\psi = \sin^{-1}(1/A_h)$ = phase angle.

Eq. (1) under the sinusoidal excitations given by Eqs. (2) and (3) was solved numerically using Runge-Kutta fourth order method. While solving Eq. (1) at each time step the impact condition ($\dot{\theta}_i * \dot{\theta}_{i+1} < 1$) is checked. If the condition is satisfied, the velocity after impact ($\dot{\theta}_{i+1}$) is modified using coefficient of restitution (e) [5], according to Eq. (4), to account for energy loss during impact (i.e., damping). From the obtained solution phase-space plot, Fourier spectra, and Poincaré sections were then plotted. Figs. 13 and 14 show the three plots for

Cask I and Cask II specimens respectively. The figures show that for the given input parameters, the response of such free-standing bodies are chaotic in nature. This means that a slight change in the initial condition or excitation parameters could result in a very different response.

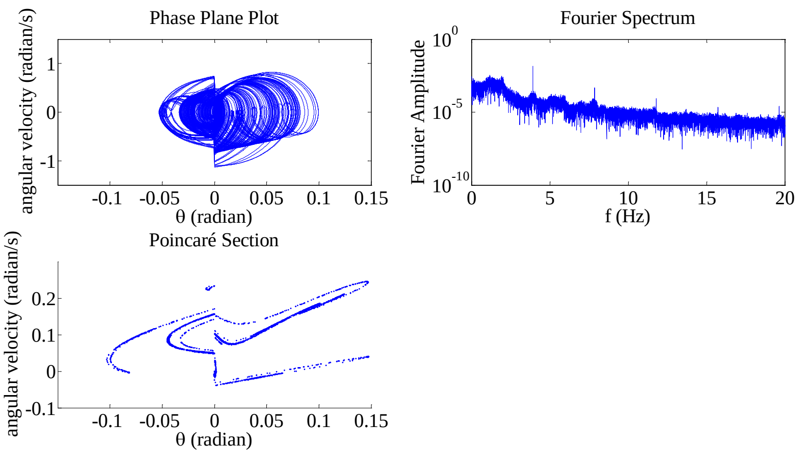

Fig. 13 – Chaotic response of Cask I (r/h_{cg} = 0.55, A_h = 3.0, A_v = 2.5, ω = 10*p, e = 0.655)

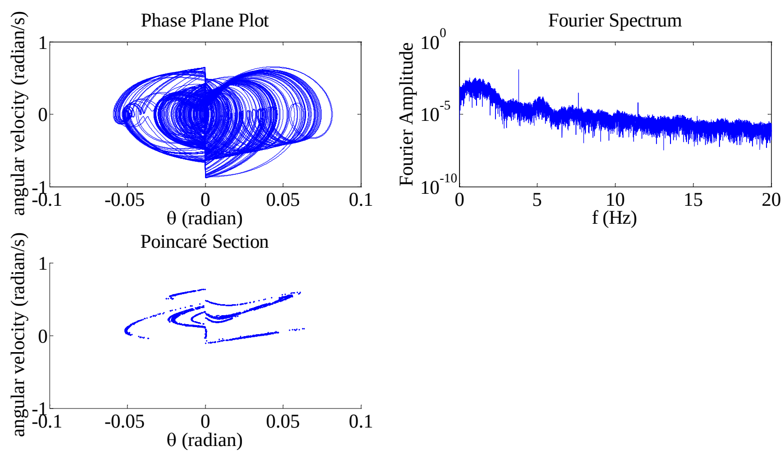

Fig. 14 – Chaotic response of Cask II (r/h_{cg} = 0.43, A_h = 3.0, A_v = 2.5, ω = 10*p, e = 0.755)

6. Conclusions

Experimental tests on scaled free-standing casks were carried out subjected to multi-directional earthquake motions. The specimens used in this study have aspect ratios of 0.62, 0.55, 0.43 and 0.39 with their respective scaling ratios. Ground motions used for the study have near field and far field characteristics. The experimental results show that FFGM with multiple pulses leads to larger rocking and lateral displacements compared to NFGM with a one or two large pulses. The series of pulses in FFGMs increases rocking and tumbling motion of the free-standing bodies as the input motion unfolds. Early pulses cause the free-standing casks to rock or tumble, making easier for the casks to move (lateral or rocking motion) when subsequent pulses occur. Ground motions were also applied multiple time to investigate whether the response of free-standing bodies is repeatable under the same ground motion. The results show that the response of the cask lacks repeatability under random input motions. A small change in initial conditions, or boundary conditions, in combination with the high frequencies contained within the applied ground motions causes a relatively large variation in the response. Despite the fact of having varied cask response, the general response under FFGM consistently shows that the multiple pulses contained in far field motion lead to larger displacements of such free-standing bodies. Finally, three methods of chaotic analysis (2D rocking only condition) were applied for Cask I and Cask II specimens.

The analysis shows that under given parameters the free-standing bodies may exhibit chaotic behaviour, and more studies are currently underway.

6. Acknowledgements

This material is based upon work supported under a Department of Energy Nuclear Energy University Programs. Any opinions, findings, conclusions or recommendations expressed in this publication are those of the authors and do not necessarily reflect the views of the Department of Energy Office of Nuclear Energy.

7. Copyrights

16WCEE-IAEE 2016 reserves the copyright for the published proceedings. Authors will have the right to use content of the published paper in part or in full for their own work.

8. References

[1] Hao H, Zhou Y (2012): Dynamic Response of Rigid Blocks to Simultaneous Horizontal and Vertical Ground Shock. *Advances in Structural Engineering*, **15**(7), 1069–1082.

[2] Makris N, Zhang J (1999). *Rocking Response and Overturning of Anchored Equipment under Seismic Excitations Rocking Response and Overturning of Anchored Equipment under Seismic Excitations*. PEER Report 1999/06, University of California, Berkeley.

[3] Dangol S, Ibarra L, Maree A, Nielsen T, Sanders D, Pantelides C (2016): Experimental Seismic Response of Scaled Storage Containments under Identical Loading Conditions. *WM2016 Conference*, Phoenix, Arizona.

[4] Luk VK, Spencer BW, Lam IP, Dameron RA (2005): *Parametric Evaluation of Seismic Behavior of Freestanding Spent Fuel Dry Cask Storage Systems*. Prepared for the Nuclear Regulatory Commission, NUREG/CR-6865, Washington DC.

[5] Housner GW (1963): The Behavior of Inverted Pendulum Structures during Earthquakes. *Bulletin of the Seismological Society of America*, **53**(2), 403–417.

[6] Yim CS, Chopra AK, Penzien J (1980): Rocking response of rigid blocks to earthquakes. *Earthquake Engineering & Structural Dynamics*, **8**(6), 565–587.

[7] Ishiyama Y (1982): Motions of Rigid Bodies and Criteria for Overturning By Earthquake Excitations. *Earthquake Engineering & Structural Dynamics*, **10**, 635–650.

[8] Mcguire RK, Silva WJ, Costantino CJ (2001):. *Technical Basis for Revision of Regulatory Guidance on Design Ground Motions: Hazard- and Risk-consistent Ground Motion Spectra Guidelines*. Prepared for the Nuclear Regulatory Commission, NUREG/CR-6728, Washington DC.

[9] Abrahamson NA (1993): *Nonstationary spectral matching program RSPMATCH*. PG&E Internal Report.

[10] Moncarz PD, Krawinkler H (1982): Similitude Requirements for Dynamic Models. *ACI Special Publication*, **73**.

[11] Dangol S, Ibarra L (2013): Effect of Vertical Accelerations on Dry Storage Cask Seismic Performance. *Smirt-22*, San Francisco, CA.

[12] Aslam M, Scalise DT, Godden WG (1980): Earthquake rocking response of rigid bodies. *Journal of the Structural Division*, **106**(2), 377–392.

[13] Hogan SJ (1990): The many steady state responses of a rigid block under harmonic forcing. *Earthquake Engineering and Structural Dynamics*; **19**(7), 1057–1071.

[14] Jeong M, Suzuki K, Yim SCS (2003): Chaotic rocking behavior of freestanding objects with sliding motion. *Journal of Sound and Vibration*, **262**(5), 1091–1112.

[15] Peña F, Prieto F, Lorenço P, Campos CA, Lemos J (2007). On the dynamics of rocking motion of single rigid-block structures. *Earthquake Engineering and Structural Dynamics*, **36**, 2382–2399.

[16] Moon FC (1992): *Chaotic and Fractal Dynamics*. John Wiley & Sons, Inc.